Moradi et al., *BioImpacts.* 2024;14(3):27510
doi: 10.34172/bi.2023.27510
https://bi.tbzmed.ac.ir/

Poly (acrylic acid)/tricalcium phosphate nanoparticles scaffold enriched with exosomes for cell-free therapy in bone tissue engineering: An *in vivo* evaluation

Nahid Moradi[1], Mina Soufi-Zomorrod[1*], Simzar Hosseinzadeh[2,3], Masoud Soleimani[1,3]

[1]Hematology and Cell Therapy Department, Faculty of Medical Sciences, Tarbiat Modares University, Tehran, Iran
[2]Medical Nanotechnology and Tissue Engineering Research Center, Shahid Beheshti University of Medical Sciences, Tehran, Iran
[3]Department of Tissue Engineering and Applied Cell Sciences, School of Advanced Technologies in Medicine, Shahid Beheshti University of Medical Sciences, Tehran, Iran

Article Info

Article Type:
Original Article

Article History:
Received: 4 Jul. 2022
Revised: 9 Dec. 2022
Accepted: 30 Jan. 2023
ePublished: 19 Jul. 2023

Keywords:
UCMSC-exosome, Critical-sized bone defect, PAA, Tricalcium phosphate nanoparticles, Cell-free therapy, Preclinical imaging

Abstract

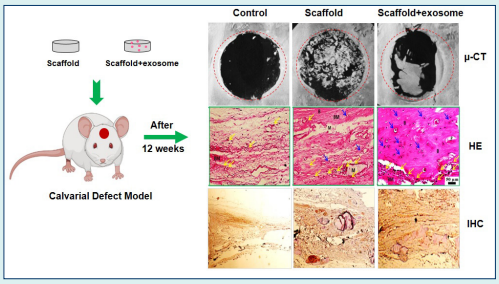

Introduction: This study aimed to assess the potential of poly (acrylic acid)/tricalcium phosphate nanoparticles (PAA/triCaPNPs) scaffold in terms of biocompatibility and osteoconductivity properties the in-vivo evaluation as well as to investigate the performance of PAA/triCaPNPs scaffold (with or without exosomes derived from UC-MSCs) for bone regeneration of rat critical-sized defect.

Methods: PAA/triCaPNPs scaffold was made from acrylic acid (AA) monomer, N,N'-methylenebisacrylamide (MBAA), sodium bicarbonate (SBC), and ammonium persulfate (APS) through freeze-drying method. For *in vivo* evaluation, we randomly divided 24 rats into three groups. The rat calvarial bone defects were treated as follows: (1) Control group: defects without any treatment, (2) scaffold group: defects treated with scaffold only, (3) scaffold+exo group: defects treated with scaffold enriched with exosomes (1 μg/μL, 150 μg per rat). Eight- and 12-weeks post-surgery, half of the animals were sacrificed and bone regeneration was examined through micro-computerized tomography (μ-CT), histological staining, and immunohistochemistry (IHC).

Results: Quantitative analysis based on μ-CT scan images at 8 and 12 weeks post-implantation clearly indicated that healing rate for defects that were filled with scaffold enriched with exosome was significantly higher than defects filled with scaffold without exosome. The H&E and Masson staining results revealed that more new bone-like form developed in the scaffold+exo group than that in control and scaffold groups. Further, IHC staining for osteocalcin and CD31 confirmed that more bone healing in the scaffold+exo group at 12 weeks could be associated with osteogenesis and angiogenesis concurrently.

Conclusion: In the present study, we aimed to investigate the therapeutic potential of PAA/triCaPNPs scaffold as a carrier of human UC-MSC-derived exosome to achieve the exosome-controlled release on calvarial bone defect. The *in vivo* results indicated that the exosome-enriched scaffold could effectively minify the defect area and improve the bone healing in rat model, and as such it could be an option for exosome-based therapy.

Introduction

Non-self-healing lesions are known as critical-sized bone defects, which are the smallest size of bone defects that are not fully and naturally repaired over time and often require therapeutic interventions to initiate bone regeneration.[1-3] Efficient and effective reconstruction of bone tissue is one of challenges in orthopedic clinical therapy.[4] Bone tissue engineering based on the use of mesenchymal stem cells has been proposed as a promising therapeutic strategy in this field. Many studies have shown that bone tissue engineered based on mesenchymal stem cells has been effective in regenerating critical-sized bone

*Corresponding author: Mina Soufi-Zomorrod, Email: m.soufi@modares.ac.ir

defects and accelerating repair.[5,6] However, direct use of these cells has a number of significant limitations, such as phenotypic changes of these cells after transplantation, low efficiency homing of injected cells, and low survival of these cells in transplantation site.[6-8] Recently, cell-free therapy based on the use of exosomes has been proposed as an alternative strategy for bone defect regeneration.[7,9] Due to considering the similarity between exosomes and their source cells, these nano-sized extracellular vesicles[10] can effectively reinforce new bone regeneration as a promising treatment in bone tissue engineering.[11] Over the past decade, umbilical cord as an inexhaustible source of mesenchymal stem cells (MSCs) with easy and non-invasive access, has become a favorable cell source for tissue repair. Since there is evidence of the healing[12] and anti-inflammatory properties[13,14] of umbilical cord mesenchymal stem cell-derived exosomes, many efforts have been made to use these exosomes in tissue repair. It is essential to utilize a suitable microenvironment for exosome entrapment, since exosomes leave bone defect sites.[9] In a bone defect site, numerous efforts have been made to design three-dimensional (3D) porous scaffolds that can carry and release exosomes.[15,16] Because of their advantages, hydrogels have received extensive attention in tissue engineering,[17] and drug delivery.[18]

Many researchers are looking to design a 3D hydrogel-based scaffolds with suitable physicochemical properties (such as good porosity and mechanical features),[19,20] to accelerate new bone formation along with increasing the duration of presence of exosomes at the bone defect sites.[15] Indeed, clinical outcomes can be enhanced by 3D scaffolds prepared with appropriate biomaterials to provide a physical supporter as well as to prevent uncontrolled release of exosomes.[16]

Through mimicking the inorganic-organic construction of the bone matrix, we have recently prepared[21] a novel scaffold made from negatively charged poly (acrylic acid) (PAA) due to its carboxylic groups and tricalcium phosphate nanoparticles (triCaPNPs) via cross-linking and freeze-drying methods. A great pharmaceutical polymer, PAA-based polymers possess biodegradability, nontoxicity, biocompatibility,[22] and an excellent specific surface region that would facilitate interactions with physiological compartments.[23] For tissue engineering[24,25] and controlled protein or drug release in target tissues, PAA-based polymers have been used as a scaffold.[26-27] Calcium phosphate (CaP) as a bone substitute has been broadly utilized in clinical practice.[30] Calcium phosphate nanoparticles have demonstrated promising functional potentials in the field of nanomedicine. These nanoparticles are found in comparatively high levels in the body, especially in tooth enamel and bone. Additionally, they are osteoconductive, biodegradable, and biocompatible.[31] However, because of their unstable suspension and ease of agglomeration, pure nanoparticles cannot be used alone; thus, we incorporated these nanoparticles into the PAA polymer matrix in our previous study. Due to the presence of Ca^{2+} on triCaP nanoparticles surface,[32] we confirmed to cross-link PAA with triCaP nanoparticles via electrostatic bonding.[21]

Bone tissue scaffolds should mimic the natural bone matrix with suitable physicochemical properties.[4] Our previous study showed that PAA/triCaPNPs scaffold has 3-120 μm pore sizes and 68% porosity. Further, this scaffold has shown appropriate mechanical and wettability properties, cell attachment, as well as osteoconduction. We then evaluated the ability of the PAA/triCaPNPs scaffold to carry and release the exosomes derived from umbilical cord MSCs (UC-MSCs).

Our *in vitro* results revealed that the scaffold has the ability to carry and release the exosomes in a controlled manner (68% of the exosomes in 14 days), so for further evaluation in this study, we aimed to assess the in-vivo study of the potential of poly (acrylic acid)/tricalcium phosphate nanoparticles (PAA/triCaPNPs) scaffold in terms of biocompatibility and osteoconductivity properties. Another aim was to investigate the performance of PAA/triCaPNPs scaffold (with or without exosomes) for bone regeneration of critical-sized defect in rat model in three groups: blank group, scaffold group, and scaffold+exosome group.

Material and Methods

Scaffold preparation

The PAA/triCaPNPs scaffold was made using acrylic acid monomer (distilled AA, 2.5 mL, 1.5 M) and tricalcium phosphate nanoparticles (triCaPNPs, 75 mg) according to the protocol mentioned in our previous article.[21] Briefly, a mixed solution of AA, MBAA (0.006 mol%), NaOH (0.12 mol%), and deionized water were made, and then nanoparticles solution was added to it. Under the nitrogen atmosphere, ammonium persulfate (APS, 0.012 mol%) and sodium bicarbonate (SBC, 0.02 mol%) were added, respectively. After heating at 75 °C and washing through deionized water for 48-72 hours, the prepared scaffold was freeze-dried for 15 hours at -50 °C (Christ GAMMA 1-16 LSC Freeze Dryers).

Exosome isolation and characterization

To separate the exosomes, we followed this way: briefly, UC-MSCs were seeded in flasks and after reaching 80% confluence, the supernatant was replaced with 10% exosome-free FBS and DMEM. Every 48 h, the medium was collected, centrifuged (300 g, 10 minutes; 2000 g, 10 minutes; and 10 000 g, 30 minutes), filtered, and ultracentrifuged (100 000 g, 70 minutes, 2 times) to get exosomes. Through Pierce BCA Protein Assay Kit (Bio Basic Inc., Canada), the concentrations of exosome proteins were assessed. Western blot analysis was also performed for exosomal surface markers such as CD9 and CD81 (Abcam, UK). Results of exosome characterization were mentioned as previously reported.[21]

Assessment of exosome attachment on scaffold surface

To show the attachment of exosomes onto the surface of the PAA/triCaPNPs scaffold, we used DiI-labeled exosomes. DiI dye was applied based on the manufacturer's protocol. Labeled exosomes were seeded drop by drop onto the surface of scaffold. After incubation for 24 hours at 37 °C, images were recorded through an Olympus iX53 microscope.

Degradation behavior of scaffold

We placed dried PAA/triCaPNPs scaffold in well plates (n=3) to demonstrate the stability of the scaffold at the defect site for *in vivo* implantation. At 37 °C, the scaffold was soaked in PBS (pH=7.4), dried using a freeze dryer (Christ GAMMA 1-16 LSC Freeze Dryers), and weighed. The scaffold was periodically immersed in PBS and dried on time points (for 240 days). It is possible to determine whether it degrades after prolonged soaking in PBS based on the variation in its weight.

Preparation of experimental groups

In our previous article, *in vitro* results indicated that the exosomes released from PAA/triCaPNPs scaffold could significantly enhance the osteogenic commitment of human UC-MSCs. Here, we aimed to evaluate the performance of PAA/triCaPNPs scaffold (with or without exosomes) and its impact on repairing critical-sized bone defects when implanted into the rat calvarium bone defect model. Briefly, a steel punch was used to make a circular scaffold of 6 mm in diameter. The scaffold pieces were then sterilized by ethanol and ultraviolet light and incubated in basal medium at 37 °C for 24 hours to detect possible contamination. Due to the swelling behavior, the scaffold pieces reached our desired diameter of 8 mm. Afterwards, to prepare the combinations of scaffold/exosome, we placed the exosomes drop by drop onto the surface of scaffolds at a concentration of 1 μg/μL, 150 μg per scaffold and placed them in a humid incubator for 18 hours prior to surgery.

Animals

All animal surgeries were performed as authorized by standard guidelines approved by Medical Research Ethics Committee of Tarbiat Modares University. For this study, 24 mature and healthy male Wistar rats (2.5-month-old, 300±30 g weight) were studied. The rats were randomly divided into three groups.

Surgical procedure

For anesthetizing the rats, 20 mg/kg ketamine hydrochloride and 5 mg/kg xylazine were injected intraperitoneally at 10 minutes before surgery. The dorsal part of the skull was sterilized via povidone-iodine (50 mg/mL) and shaved. Then, the skin over the calvarium bone and the periosteum were incised at the sagittal site. In each rat, a central cranial defect (circular shape, 8 mm diameter) was created using a trephine bur (Komet Dental, Germany) under irrigating saline (0.9%) while the dura matter was not damaged. The cranial bone defects were treated as follows:

(1) Control group: defects without any treatment, *(2) scaffold group:* defects treated with PAA/triCaPNPs scaffold only, *(3) scaffold+exo group:* defects treated with PAA/triCaPNPs scaffold enriched with exosome (1 μg/μL, 150 μg per rat).[9] After implantation, the skin incision was closed with nonabsorbable sutures. Enrofloxacin (2.5 mg/kg) as an antibiotic was administered per day for 5 days. At 8 and 12 weeks post-surgery, half of the rats in each group were randomly selected and euthanized by CO2 inhalation. Then, the calvarial defect sites were harvested and fixed to 48 hours in 4% paraformaldehyde for further analysis.

μ-CT analysis

Micro-computed tomography (μ-CT) is an imaging technique using X-ray to assess the inside of critical bone defect site with the scaffold in situ, which was performed on a μ-CT scanner (LOTUS-inVivo Micro-CT Scanner, BN Imaging Technology Company, Iran) at a resolution of 15 μm, a voltage of 55 kV at a greyscale threshold of 150. Reconstructed μ-CT images were obtained by RadiAnt DICOM viewer. The bone mineral density (BMD), new bone volume fraction (BV/TV), and trabecular thickness were all calculated statistically using the μ-CT software.[33] For calculating the new bone volume in scaffold and scaffold+exo groups, the mean bone volume of the control group (without any treatment) was subtracted from them. Equivalent sites in rats were examined for standardization.[34]

Hematoxylin–Eosin and Masson's trichrome staining

For histological analysis, calvaria were decalcified in EDTA (10% w/v) at 37 °C for 28 days and then dehydrated in ethanol series. Thereafter, specimens were embedded in paraffin. The paraffin blocks were cut into 5-μm-thick sections. Subsequently, Hematoxylin–Eosin (H&E) and Masson's trichrome (Sigma Aldrich, UK) staining were performed.

Immunohistochemistry (IHC) analysis

IHC is used to detect the presence of osteocalcin (OCN: a specific protein expressed and secreted solely by osteoblasts[35]) and CD31 (a protein to demonstrate the presence of endothelial cells in histological tissue sections). The process was performed using anti-OCN antibody based on standard protocol. Briefly, the paraffin-embedded tissue samples were de-waxed and rehydrated in xylene twice for 10 min each. Then, the slides were immersed in ethanol series (100%, 95%, 70%, 50% respectively, for 5 min each) and water. After antigen retrieval and reducing endogenous peroxidase activity, the sections were subsequently incubated with

primary antibody (Anti-Osteocalcin, Abcam, ab13420, monoclonal (OCG3), diluted 1:250 and Anti-CD31, Abcam, ab281583, monoclonal, diluted 1:50) at 4 °C overnight. Next, the sections were labelled with the secondary antibody and visualized. Using ImageJ software and four slides from each group, quantitative analysis of IHC results was performed.

Data analysis

ANOVA analysis or t-test was used to assess the difference between results. All data is presented as mean ± standard deviation. Data analysis was performed through GraphPad Prism. $P < 0.05$ was considered significant.

Results

Previously we investigated the effects of the scaffold on osteogenesis *in vitro*. Compared to cells cultured on plates, UC-MSCs implanted on PAA/triCaPNPs scaffold significantly enhanced osteogenesis. We also mentioned in the previous article that the scaffold had the ability to carry and release exosomes extracted from UC-MSCs.[21] In this paper, we seek to confirm these results *in vivo*.

Structure of 3D scaffold

PAA/triCaPNPs scaffold cross-sectional thickness was prepared and observed by SEM. According to the analysis, the scaffold showed a 3D multiscale pore structure with 68% porosity[21] (Fig. 1A)

Assessment of exosome attachment on scaffold surface

To indicate the attachment of exosomes to the surface of PAA/triCaPNPs scaffold, we used DiI-labeled exosomes. After incubating for 24 hours at 37 °C, as displayed in Fig. 1B, the red-labeled vesicles are present on the surface of the scaffold, showing the ability of the exosomes to be attached onto the scaffold surface.

Degradation behavior of scaffold

To show the stability of PAA/triCaPNPs scaffold in defect site, we placed the pieces of scaffold in PBS at 37 °C for eight months. As shown in Fig. 1C, it is obvious that scaffold weight gets heavier over time up to seventh month. It's possible that the scaffold takes in PBS during soaking, and because PBS contains salts that are stored in the scaffold's pores, they accumulate and get heavier over time.

Preparation of experimental groups

The scaffold pieces with a diameter of 6 mm were sterilized and incubated in basal medium at 37 °C for 24 hours to detect possible contamination. As displayed in Fig. 2, due to the swelling behavior, the scaffold pieces reached our desired diameter of 8 mm.

The surgical procedure was performed as shown in Fig. 3A (1-5). Next, the calvarial defect sites were harvested at 8 and 12 weeks after surgery. Fig 3B displays a macroscopic view of the rat skull (defect site and almost three millimeters around the defect).

μ-CT analysis of new bone formation

As displayed in Fig. 4, the micro-CT results indicated that compared with the control group, much more new bone

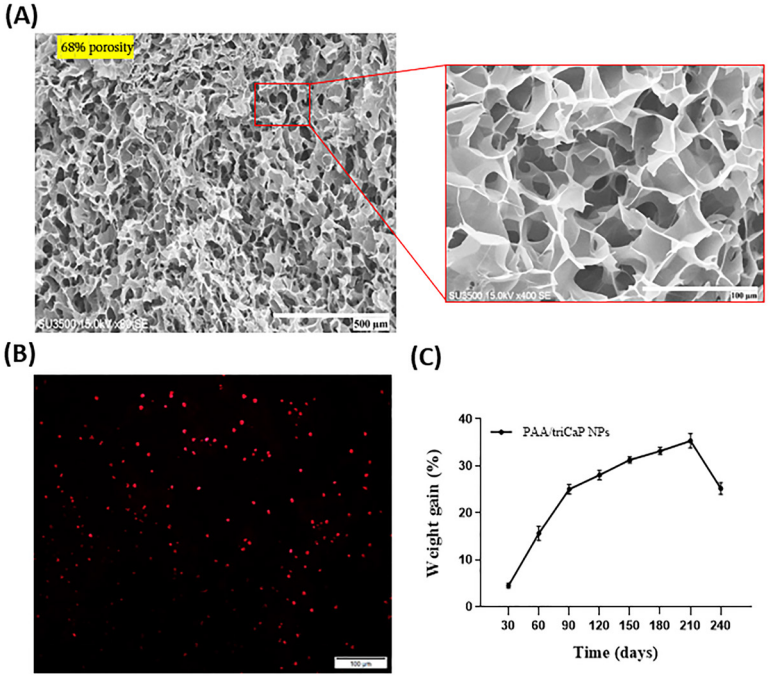

Fig. 1. SEM photograph of freeze-dried cross-section of PAA/triCaPNPs scaffold structure; scale bars: 500 and 100 μm. The scaffold shows 68 % porosity **(A)**. Photomicrograph of exosomes attached on scaffold 24 h after seeding. Exosomes stained with DiI dye; scale bars: 100 μm **(B)**. Degradation behavior of PAA/triCaPNPs scaffold in PBS at 37 °C **(C)**.

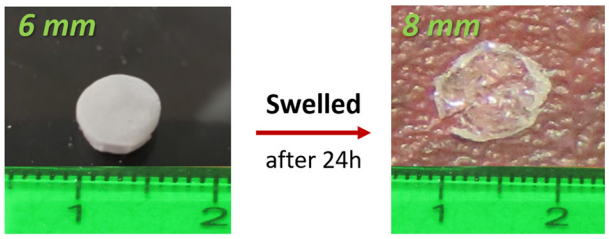

Fig. 2. Swelling behavior of PAA/triCaPNPs scaffold by passing 24 hours that it was exposed to the culture medium.

was generated in the scaffold groups. These results were clearly repeated at both timepoints. Note that according to the prediction, in the 12 weeks after surgery, the rate of new bone formation was far higher in both groups with scaffold compared to the control group, particularly in scaffold+exo group. Also, bone volume fraction (BV/TV), BMD, and trabecular thickness were calculated to the measure new bone formation rate. The results confirmed that the largest extent of new bone was formed in the scaffold+exo group three months post-implantation (Fig. 5; $P < 0.05$).

Histology staining analysis

To evaluate the new bone-like tissue formation, H&E staining was performed at 8 and 12 weeks post-surgery. As depicted in Fig. 6, deposition of new bone increased in scaffold+exo group compared with the other two groups. The Masson staining results are shown in Fig. 7. These results also represented more new bone-like form development in the scaffold+exo group than in control and scaffold groups. In the control group at both time points, more bounded connective tissue was seen rather than bone-like tissue at the edges of the defect site.

IHC analysis

To confirm the new bone-like tissue formation, IHC staining was done. A higher expression of osteogenic

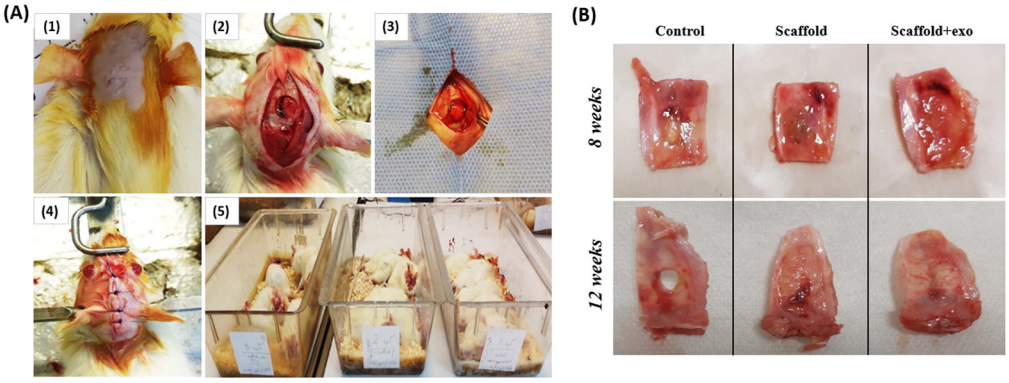

Fig. 3. Surgical procedure (A): The rat skull was sterilized and shaved (1), Skin and periosteum were slit and the skull bone was pierced using a trephine bur (2), PAA/triCaPNPs scaffold or PAA/triCaPNPs scaffold enriched with exosomes were implanted (3), Skin incision was closed (4), and Surgical rats in three groups (5); A macroscopic view of calvarial defect sites were harvested at 8 and 12 weeks after surgery (B).

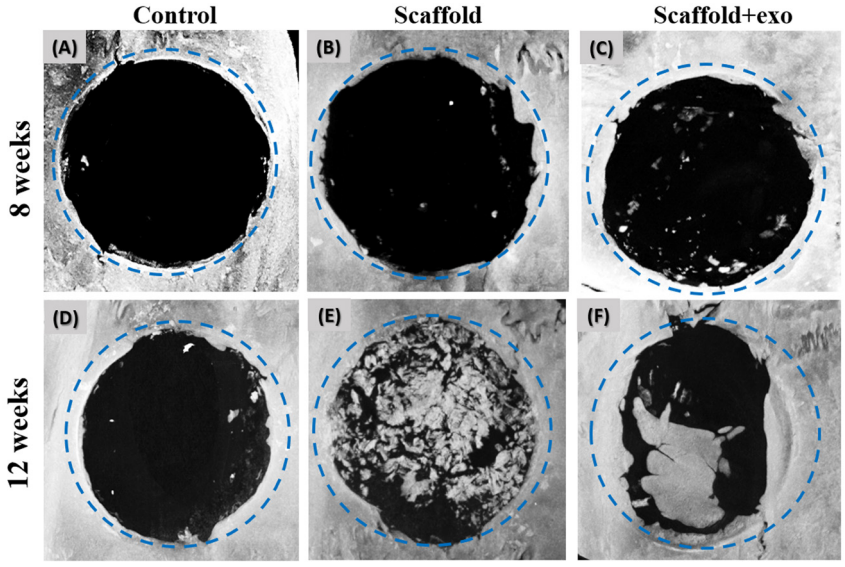

Fig. 4. Reconstructed μ-CT images at 8 (A-C) and 12 (D-F) weeks after implantation. As shown, at both points in time, the defect diameter that was implanted with PAA/triCaPNPs scaffold enriched with exosomes was clearly decreased compared to PAA/triCaPNPs scaffold and control.

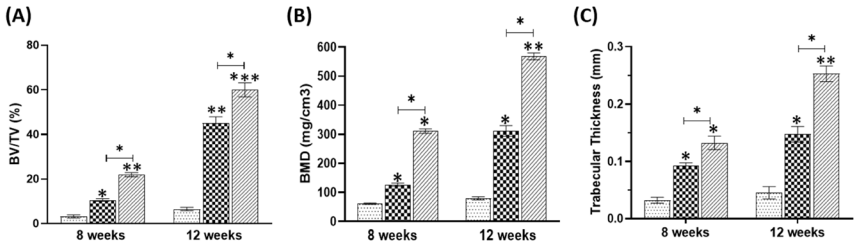

Fig. 5. Quantitative analysis of new bone formation based on μ-CT images at 8 and 12 weeks by using BV/TV (A), BMD (B), trabecular thickness (C). (*P < 0.05, ** P < 0.01, ***P<0.001).

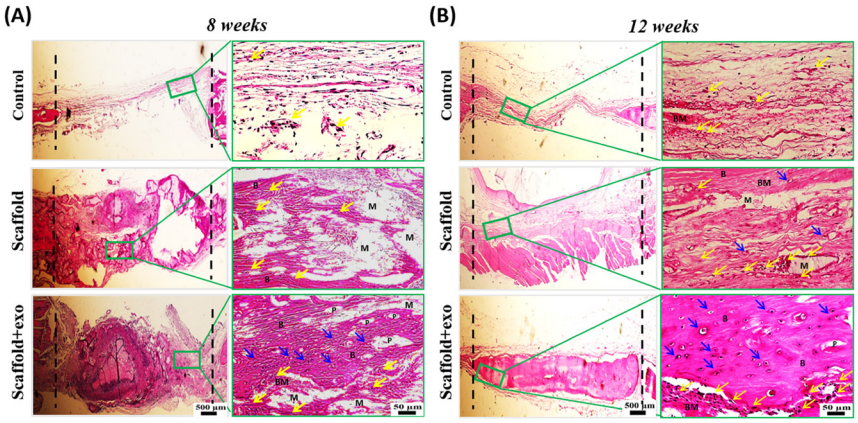

Fig. 6. Histological evaluation (HE staining) at the endpoint of 8 (A) and 12 (B) weeks; scale bars: 500 μm and 50 μm. **B:** new bone, **BM**: new bone matrix, **M:** remaining material from implanted scaffold, **P:** visible pores from implanted scaffold, **Yellow arrow**: osteoblast, **Blue arrow:** osteocyte inside lacuna.

marker (OCN) was statistically revealed in the scaffold+exo group than in the other groups (Fig. 8a,b) (P<0.05). Based on the results, over time, the difference between scaffold+exo group and other groups has increased (P<0.01). Furthermore, the expression of CD31 as a key marker for capillary endothelial cells was examined. As indicated in Fig. 8c,d, in the scaffold+exo group more CD31 positively stained cells were detected after 12 weeks than in the control and scaffold groups (P<0.05), but no significant differences were recorded between scaffold+exo and scaffold groups after 8 weeks. This suggests that more neovascularization occurred in scaffold+exo group than in the scaffold group after 12 weeks.

Discussion

Accelerating bone healing is one of the orthopedic challenges that requires further study. Although stem cell therapy has been shown to be effective, many studies have shown that paracrine functions play a role as effective mechanisms of treatment.[9,36] Numerous studies have reported that exosomes, as nanocarriers of biological biomolecules,[10,37] are the major paracrine factors secreted by mesenchymal stem cells that have impressive effects on tissue regeneration.[7,38] Easy and non-invasive access to the umbilical cord as a source of MSCs,[39] as well as good proliferative properties and high differentiation capacity,[40,41] make these cells a reliable source for exosome extraction. Previous studies have found that human UC-MSCs, like bone marrow MSCs, promote bone differentiation in a bone defect animal model.[42,43]

Exosomes leave the bone site defect quickly if they are directly injected at site. As such, many studies have aimed to prepare a scaffold using suitable biomaterials for entrapping, prolonging their presence, as well as action time and, thus, to reinforce their positive effects.[9,15,44]

We have prepared a novel scaffold (PAA/triCaPNP) by the cross-linking method as described.[21] Now, this study aims to assess the potentials of the new 3D scaffold with and without exosomes for bone regeneration in calvarial defect animal models.

The scaffold was observed for eight months in PBS at 37 °C to determine whether it could be implanted into the human body for an extended period of time without degrading.[45] The scaffold begins to degrade in the seventh month, but before that, the weight of the scaffold increased. It is thought that the PAA slowly hydrolyzes in PBS, which is the cause. Water molecules easily penetrate the polymer network because of the structure of the pores. The hydrolytic groups in PAA make it easy for the water molecules to be absorbed onto the scaffold surface. Hydrolysis results in the dissociation of the bonds after that. As a result, molecular structure collapse may also disrupt the crosslinks between molecules and the

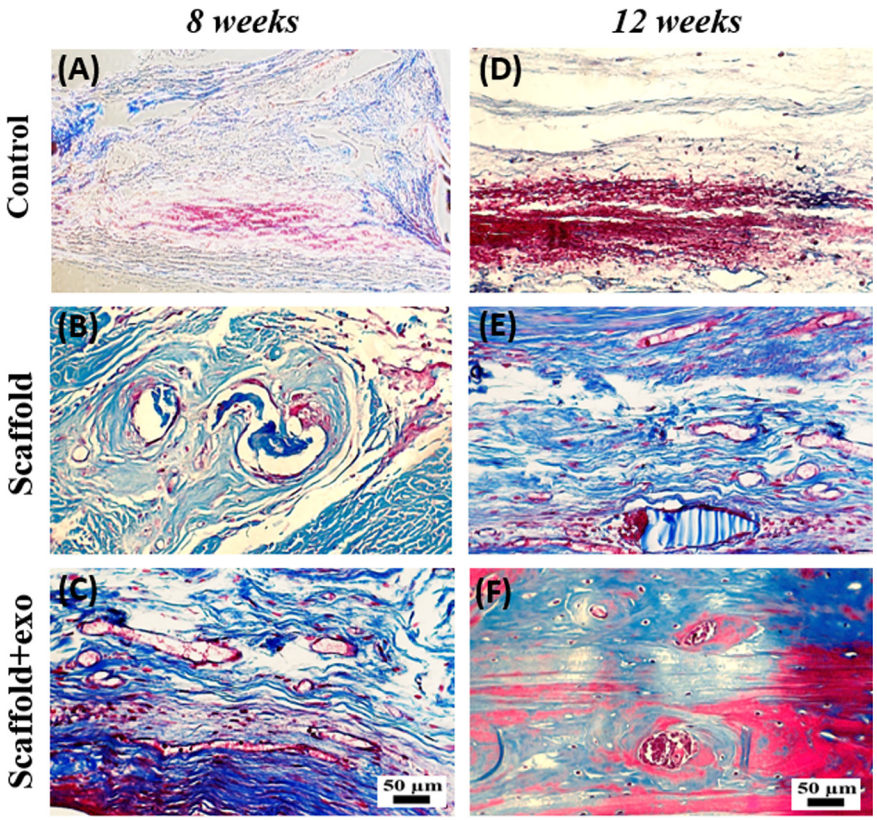

Fig. 7. Histological evaluation (Masson's Trichrome staining) at the endpoint of 8 (A-C) and 12 (D-F) weeks; scale bar: 50 µm

electrostatic force between PAA and Ca^{2+}.[45, 46] Because of this, it has been confirmed that this scaffold covers the bone tissue's period of repair.

Qualitatively, in comparison with control, the 3D reconstructed micro-CT scan images showed that some new bone was formed inside of defects in both groups that were filled with the PAA/triCaPNPs scaffold, while in the control group, new bone was formed only at the margin of the defect. This result well indicated that the prepared scaffold provided a suitable platform for bone ingrowth. These observations were completely consistent with the results obtained from the in vitro study. In other words, the 3D microenvironment with interconnected porosity provided by the PAA/triCaPNPs scaffold could help improve the osteoconductive capability which leads to micronutrient directing, cell recruitment, migration, proliferation, and differentiation.[4,31,47] Based on our previous study, the pore size range of PAA/triCaPNPs scaffold was within 3-120 µm. In the literature, in a bone scaffold, 5 µm for new functional microvascular networks and 40-100 µm for osteoid formation have been suggested as the optimal pore size range[4]: thus, a multiscale porous structure of this scaffold provides a suitable substrate to form more new bone in the groups filled with scaffold, compared with the control group.

Further, quantitative analysis based on CT scan images at 8 and 12 weeks after implantation clearly indicated that healing rate for defects filled with scaffold enriched with exosome was significantly higher than defects filled with scaffolds without exosome ($P<0.05$). As displayed in Fig. 5, BV/TV, BMD, and trabecular thickness in the scaffold+exo group increased by 2.6-fold, 3.7-fold, and 2-fold respectively ($P<0.05$) compared to that in the scaffold group at 8 weeks and 2.4-fold, 2.2-fold, and 1.7-fold respectively ($P<0.05$) at 12 weeks after implantation. According to the results of µ-CT scan analysis and histological examinations, the exosomes released from the scaffold have been able to play an effective role in promoting repair at the bone defect site in the rat model. Thus, the results of the current study are consistent with studies that examined the effect of exosomes extracted from UC-MSCs on bone repair.[12,48] For example, Wang and colleagues[49] prepared a coralline hydroxyapatite (CHA)/silk fibroin (SF)/glycol chitosan (GCS)/difunctionalized polyethylene glycol (DF-PEG) self-healing hydrogel. They showed bone regeneration levels in hydrogel containing exosomes were significantly higher than those of the hydrogel and control groups. Zhou et al[50] focused on evaluating the mechanism of osteogenesis by human UCMSC-derived exosomes. They injected PBS or exosomes at the fracture site in SD rats. According to the Western Blotting results, the expression levels of β-catenin and Wnt3a in the exosome-treated group were significantly higher than those in the control group and PBS injection group ($P < 0.01$). So, they deduced that these exosomes are involved in bone healing through the Wnt signaling pathway.

Previous studies have shown that the action underlying mechanisms of exosomes secreted from human UCMSC

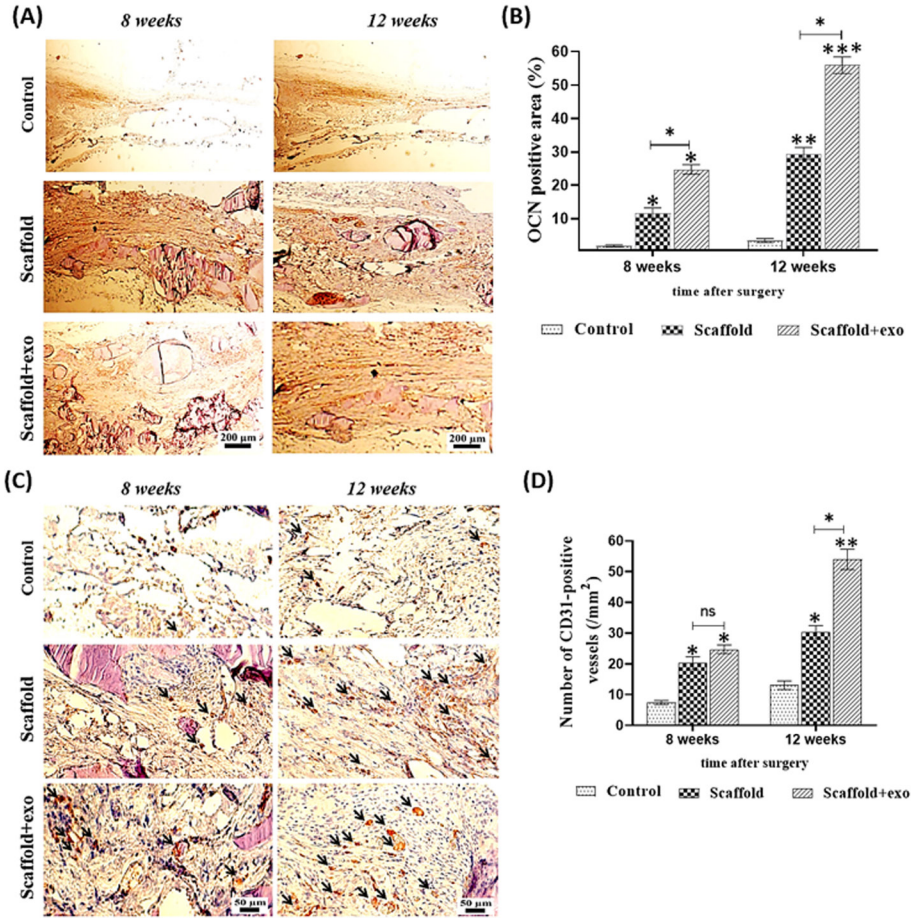

Fig. 8. Assessment of expression of osteocalcin (OCN) in rat calvarial defects at 8- and 12-weeks post-surgery using immunohistochemical staining (A), Quantitative analysis of OCN expression (B). Assessment of expression of CD31 in rat calvarial defects at 8- and 12-weeks post-surgery using immunohistochemical staining, black arrows show the blood vessels suggesting that more neovascularization occurred in the scaffold-exo group than in the other groups (C), Quantitative analysis of CD31 expression (D) (*P < 0.05, ** P < 0.01, ***P<0.001).

as an intercellular messenger may be related to increasing expression of hypoxia-inducible factor-1α[51] (HIF-1α: as mediator of promotion of angiogenesis), BMP-2, and VEGF in target cells.[52] In addition, it was demonstrated that exosomes secreted from human UCMSC were able to improve vascularization at the wound site by the Wnt4 protein (as a protein present in UCMSC-Exos), which can stimulate Wnt/β-catenin pathway in endothelial cells.[36]

Here, in line with other articles, by comparing the results in the two groups of scaffold+exo and scaffold, we confirmed the great biological role of UCMSC-Exos in healing the bone defect site. As depicted in Fig. 8 in the scaffold+exo group, more OCN stained area was detected after 8 and 12 weeks than that in the scaffold group (*$P<0.05$), suggesting osteogenesis activities of the exosomes-enriched scaffold to improve the bone regeneration. Also, in the scaffold+exo group, more CD31 positively stained cells were detected at 12 weeks than in the scaffold group, suggesting more neovascularization occurred due to exosome presence ($P<0.05$). However, at 8 weeks, no significant differences were recorded between these two groups. As such, IHC staining for osteocalcin (as a specific bone marker) and CD31 (as a key marker for capillary endothelial cells) confirmed that more bone healing in the scaffold+exo group at 12 weeks could be associated with osteogenesis and angiogenesis concurrently.

Due to the presence of tricalcium phosphate nanoparticles in PAA/triCaPNPs scaffold, we previously verified[21] that the physicochemical properties of PAA polymer were improved in favor of osteogenic differentiation. Nanoparticles can improve the surface roughness of scaffolds, which often correlates with marked changes in cell bioactivities, cell morphology, and the secretion of regulatory factors.[53] In general, surface roughness develops cell attachment, cell migration, and ECM production.[54] Thus, it seems that tricalcium phosphate nanoparticles have increased the surface roughness of PAA; besides electrostatic interactions, surface roughness can lead to increased likelihood of the exosome interaction with the PAA/triCaPNPs scaffold.

The study limitations included the unknown exact mechanism of osteogenesis of exosome-enriched scaffold as well as the exact mechanism of interaction between exosomes and PAA/triCaPNPs scaffold which certainly warrants further study.

Research Highlights

What is the current knowledge?

√ PAA/triCaPNPs scaffold has excellent physicochemical properties that improves osteogenic differentiation *in vitro.*

√ This scaffold can carry and release exosomes in functional form into the medium.

What is new here?

√ The exosome-enriched PAA/triCaPNPs scaffold indicates an effective role for exosome-based therapy *in vivo* and could be a promising strategy for bone tissue engineering.

Conclusion

This study aimed to investigate the therapeutic potential of PAA/triCaPNPs scaffold as a carrier of human UC-MSC-derived exosome to achieve the exosome-controlled release on calvarial bone defect in animal models. The *in vivo* results revealed that the exosome-enriched scaffold could effectively minify the defect area and improve the bone healing in the rat model, so it could be an option for exosome-based therapy.

Acknowledgments

We thank the Preclinical Core Facility of Tehran University of Medical Sciences to provide excellent facilities for micro-CT imaging.

Authors' contribution

Conceptualization: Nahid Moradi, Mina Soufi-Zomorrod.
Data curation: Nahid Moradi.
Formal analysis: Nahid Moradi.
Funding acquisition: Nahid Moradi, Mina Soufi-Zomorrod.
Investigation: Nahid Moradi.
Methodology: Nahid Moradi, Simzar Hosseinzadeh.
Project administration: Mina Soufi-Zomorrod.
Resources: Mina Soufi-Zomorrod.
Software: Nahid Moradi.
Supervision: Mina Soufi-Zomorrod, Masoud Soleimani.
Validation: Nahid Moradi.
Visualization: Nahid Moradi.
Writing–original draft: Nahid Moradi.
Writing–review & editing: Masoud Soleimani.

Competing Interests

There is no competing financial interest.

Ethical Statement

Tarbiat Modares University's Medical Research Ethics Committee (IR.MODARES.REC.1398.093) was confirmed this study.

Funding

Council for Development of Stem Cell Sciences and Technologies, Grant/Award Number: 11/37701.

References

1. Zhao Y, Li Z, Jiang Y, Liu H, Feng Y, Wang Z, *et al.* Bioinspired mineral hydrogels as nanocomposite scaffolds for the promotion of osteogenic marker expression and the induction of bone regeneration in osteoporosis. *Acta Biomaterialia* **2020**; 113: 614-26 .https://doi.org/10.1016/j.actbio.2020.06.024
2. Finkemeier CG. Bone-grafting and bone-graft substitutes. *J Bone Joint Surg Am* **2002**; 84: 454-64. https://doi.org/10.2106/00004623-200203000-00020
3. Gomes KU, Carlini JL, Biron C, Rapoport A, Dedivitis RA. Use of allogeneic bone graft in maxillary reconstruction for installation of dental implants. *J Oral Maxillofac Surg* **2008**; 66: 2335-8. https://doi.org/10.1016/j.joms.2008.06.006
4. Henkel J, Woodruff MA, Epari DR, Steck R, Glatt V, Dickinson IC, *et al.* Bone Regeneration Based on Tissue Engineering Conceptions — A 21st Century Perspective. *Bone Res.* **2013**; 1: 216-48. https://doi.org/10.4248/BR20130300 .
5. Wiltfang J, Zernial O, Behrens E, Schlegel A, Warnke PH, Becker ST. Regenerative treatment of peri-implantitis bone defects with a combination of autologous bone and a demineralized xenogenic bone graft: a series of 36 defects. *Clin Implant Dent Relat Res* **2012**; 14: 421-7. https://doi.org/10.1111/j.1708-8208.2009.00264.x
6. Djouad F, Bouffi C, Ghannam S, Noël D, Jorgensen C. Mesenchymal stem cells: innovative therapeutic tools for rheumatic diseases. *Nat Rev Rheumatol* **2009**; 5: 392-9. https://doi.org/10.1038/nrrheum.2009.104
7. Baglio SR, Pegtel DM, Baldini N. Mesenchymal stem cell secreted vesicles provide novel opportunities in (stem) cell-free therapy. *Front Physiol* **2012**; 3: 359. https://doi.org/10.3389/fphys.2012.00359
8. Bruno S, Collino F, Tetta C, Camussi G. Dissecting paracrine effectors for mesenchymal stem cells. *Adv Biochem Eng Biotechnol* **2013**; 129: 137-52. https://doi.org/10.1007/10_2012_149
9. Yang S, Zhu B, Yin P, Zhao L, Wang Y, Fu Z, *et al.* Integration of Human Umbilical Cord Mesenchymal Stem Cells-Derived Exosomes with Hydroxyapatite-Embedded Hyaluronic Acid-Alginate Hydrogel for Bone Regeneration. *ACS Biomater Sci Eng* **2020**; 6: 1590-602. https://doi.org/10.1021/acsbiomaterials.9b01363
10. Beit-Yannai E, Tabak S, Stamer WD. Physical exosome: exosome interactions. *J Cell Mol Med* **2018**; 22: 2001-6.
11. Hade MD, Suire CN, Suo Z. Mesenchymal Stem Cell-Derived Exosomes: Applications in Regenerative Medicine. *Cells* **2021**; 10: 1959.
12. Wang K-X, Xu L-L, Rui Y-F, Huang S, Lin S-E, Xiong J-H, *et al.* The effects of secretion factors from umbilical cord derived mesenchymal stem cells on osteogenic differentiation of mesenchymal stem cells. *PloS One* **2015**; 10: e0120593-e. https://doi.org/10.1371/journal.pone.0120593
13. Liang L, Wang L, Zhou S, Li J, Meng L, Zhang H, *et al.* Exosomes derived from human umbilical cord mesenchymal stem cells repair injured endometrial epithelial cells. *J Assist Reprod Genet* **2020**; 37: 395-403. https://doi.org/10.1007/s10815-019-01687-4
14. Mao F, Wu Y, Tang X, Kang J, Zhang B, Yan Y, *et al.* Exosomes Derived from Human Umbilical Cord Mesenchymal Stem Cells Relieve Inflammatory Bowel Disease in Mice. *BioMed Res Int* **2017**; 2017: 5356760-. https://doi.org/10.1155/2017/5356760
15. Zhang J, Liu X, Li H, Chen C, Hu B, Niu X, *et al.* Exosomes/tricalcium phosphate combination scaffolds can enhance bone regeneration by activating the PI3K/Akt signaling pathway. *Stem Cell Res Ther* **2016**; 7: 136. https://doi.org/10.1186/s13287-016-0391-3
16. Gandolfi MG, Gardin C, Zamparini F, Ferroni L, Esposti MD, Parchi G, *et al.* Mineral-Doped Poly(L-lactide) Acid Scaffolds Enriched with Exosomes Improve Osteogenic Commitment of Human Adipose-Derived Mesenchymal Stem Cells. *Nanomaterials (Basel)* **2020**; 10: 432. https://doi.org/10.3390/nano10030432.
17. Huang K, Wu J, Gu Z. Black Phosphorus Hydrogel Scaffolds Enhance Bone Regeneration via a Sustained Supply of Calcium-Free Phosphorus. *ACS Appl Mater Interfaces* **2019**; 11: 2908-16. https://doi.org/10.1021/acsami.8b21179
18. Argentiere S, Blasi L, Ciccarella G, Barbarella G, Cingolani R, Gigli G. Nanogels of poly(acrylic acid): Uptake and release behavior with fluorescent oligothiophene-labeled bovine serum albumin. *J Appl Polym Sci* **2010**; 116: 2808-15. https://doi.org/https://doi.org/10.1002/app.31691

19. Zhu L, Luo D, Liu Y. Effect of the nano/microscale structure of biomaterial scaffolds on bone regeneration. *J Appl Polym Sci* **2020; 12:6.** https://doi.org/10.1038/s41368-020-0073-y
20. Jenkins TL, Little D. Synthetic scaffolds for musculoskeletal tissue engineering: cellular responses to fiber parameters. *NPJ Regen Med* **2019**; 4: 15. https://doi.org/10.1038/s41536-019-0076-5
21. Moradi N, Kaviani S, Soufizomorrod M, Hosseinzadeh S, Soleimani M. Preparation of poly(acrylic acid)/tricalcium phosphate nanoparticles scaffold: Characterization and releasing UC-MSCs derived exosomes for bone differentiation. *Bioimpacts* 2023; 13: 425-438. https://doi.org/10.34172/bi.2022.24142
22. Swift T, Swanson L, Geoghegan M, Rimmer S. The pH-responsive behaviour of poly(acrylic acid) in aqueous solution is dependent on molar mass. *Soft Matter* **2016**; 12: 2542-9. https://doi.org/10.1039/C5SM02693H
23. des Rieux A, Fievez V, Garinot M, Schneider YJ, Préat V. Nanoparticles as potential oral delivery systems of proteins and vaccines: a mechanistic approach. *J Control Release* **2006**; 116: 1-27. https://doi.org/10.1016/j.jconrel.2006.08.013
24. Pourbashir S, Shahrousvand M, Ghaffari M. Preparation and characterization of semi-IPNs of polycaprolactone/poly (acrylic acid)/cellulosic nanowhisker as artificial articular cartilage. *Int J Biol Macromol* **2020**; 142: 298-310.
25. Zhang Y, Wu H, Yuan B, Zhu X, Zhang K, Zhang X. Enhanced osteogenic activity and antibacterial performance in vitro of polyetheretherketone by plasma-induced graft polymerization of acrylic acid and incorporation of zinc ions. *J Mater Chem B* **2021;** 9: 7506-15. https://doi.org/10.1039/D1TB01349A
26. Ayers D, Cuthbertson JM, Schroyer K, Sullivan SM. Polyacrylic acid mediated ocular delivery of ribozymes. *J Control Release* **1996**; 38: 167-75.
27. Hajikhani M, Khanghahi MM, Shahrousvand M, Mohammadi-Rovshandeh J, Babaei A, Khademi SMH. Intelligent superabsorbents based on a xanthan gum/poly (acrylic acid) semi-interpenetrating polymer network for application in drug delivery systems. *Int J Biol Macromol* **2019**; 139: 509-20.
28. Wang X, Zhang M, Zhang L, Li L, Li S, Wang C, *et al.* Designed Synthesis of Lipid-Coated Polyacrylic Acid/Calcium Phosphate Nanoparticles as Dual pH-Responsive Drug-Delivery Vehicles for Cancer Chemotherapy. *Chemistry* **2017**; 23: 6586-95. https://doi.org/10.1002/chem.201700060
29. Li L, Zhang L, Wang T, Wu X, Ren H, Wang C, *et al.* Facile and Scalable Synthesis of Novel Spherical Au Nanocluster Assemblies@ Polyacrylic Acid/Calcium Phosphate Nanoparticles for Dual-Modal Imaging-Guided Cancer Chemotherapy. *Small* **2015**; 11: 3162-73. https://doi.org/10.1002/smll.201403517
30. LeGeros RZ. Calcium phosphate-based osteoinductive materials. *Chem Rev* **2008**; 108: 4742-53. https://doi.org/10.1021/cr800427g
31. Bose S, Tarafder S. Calcium phosphate ceramic systems in growth factor and drug delivery for bone tissue engineering: A review. *Acta Biomaterialia* **2012**; 8: 1401-21. https://doi.org/10.1016/j.actbio.2011.11.017
32. Lin K, Xia L, Gan J, Zhang Z, Chen H, Jiang X, *et al.* Tailoring the nanostructured surfaces of hydroxyapatite bioceramics to promote protein adsorption, osteoblast growth, and osteogenic differentiation. *ACS Appl Mater Interfaces* **2013**; 5: 8008-17. https://doi.org/10.1021/am402089w
33. Cukjati D, Reberšek S, Miklavčič D. A reliable method of determining wound healing rate. *Med Biol Eng Comput* **2001**; 39: 263-71. https://doi.org/10.1007/BF02344811
34. Spicer PP, Kretlow JD, Young S, Jansen JA, Kasper FK, Mikos AG. Evaluation of bone regeneration using the rat critical size calvarial defect. *Nat Protoc* **2012**; 7: 1918-29. https://doi.org/10.1038/nprot.2012.113
35. Hauschka PV, Lian JB, Cole DE, Gundberg CM. Osteocalcin and matrix Gla protein: vitamin K-dependent proteins in bone. *Physiol Rev* **1989**; 69: 990-1047. https://doi.org/10.1152/physrev.1989.69.3.990
36. Zhang B, Wu X, Zhang X, Sun Y, Yan Y, Shi H, *et al.* Human Umbilical Cord Mesenchymal Stem Cell Exosomes Enhance Angiogenesis Through the Wnt4/β-Catenin Pathway. *Stem Cells Transl Med* **2015**; 4: 513-22. https://doi.org/10.5966/sctm.2014-0267
37. Bhome R, Del Vecchio F, Lee G-H, Bullock MD, Primrose JN, Sayan AE, *et al.* Exosomal microRNAs (exomiRs): Small molecules with a big role in cancer. *Cancer Lett* **2018**; 420: 228-35. https://doi.org/10.1016/j.canlet.2018.02.002
38. Girón J, Maurmann N, Pranke P. The role of stem cell-derived exosomes in the repair of cutaneous and bone tissue. *J Cell Biochem* **2022**; 123: 183-201. https://doi.org/10.1002/jcb.30144
39. Anonymous. Transplanted Umbilical Cord Mesenchymal Stem Cells Modify the In Vivo Microenvironment Enhancing Angiogenesis and Leading to Bone Regeneration. *Stem Cells Dev* **2015**; 24: 1570-81. https://doi.org/10.1089/scd.2014.0490
40. Cheng H, Qiu L, Ma J, Zhang H, Cheng M, Li W, *et al.* Replicative senescence of human bone marrow and umbilical cord derived mesenchymal stem cells and their differentiation to adipocytes and osteoblasts. *Mol Biol Rep* **2011**; 38: 5161-8. https://doi.org/10.1007/s11033-010-0665-2
41. Deuse T, Stubbendorff M, Tang-Quan K, Phillips N, Kay MA, Eiermann T, *et al.* Immunogenicity and immunomodulatory properties of umbilical cord lining mesenchymal stem cells. *Cell Transplant* **2011**; 20: 655-67. https://doi.org/10.3727/096368910x53647 .
42. Schneider RK, Puellen A, Kramann R, Raupach K, Bornemann J, Knuechel R, *et al.* The osteogenic differentiation of adult bone marrow and perinatal umbilical mesenchymal stem cells and matrix remodelling in three-dimensional collagen scaffolds. *Biomaterials* **2010**; 31: 467-80. https://doi.org/10.1016/j.biomaterials.2009.09.059
43. Chen W, Liu J, Manuchehrabadi N, Weir MD, Zhu Z, Xu HH. Umbilical cord and bone marrow mesenchymal stem cell seeding on macroporous calcium phosphate for bone regeneration in rat cranial defects. *Biomaterials* **2013**; 34: 9917-25. https://doi.org/10.1016/j.biomaterials.2013.09.002
44. Li W, Liu Y, Zhang P, Tang Y, Zhou M, Jiang W, *et al.* Tissue-Engineered Bone Immobilized with Human Adipose Stem Cells-Derived Exosomes Promotes Bone Regeneration. *ACS Appl Mater Interfaces* **2018**; 10: 5240-54. https://doi.org/10.1021/acsami.7b17620
45. Lin Y-J, Hsu F-C, Chou C-W, Wu T-H, Lin H-R. Poly(acrylic acid)–chitosan–silica hydrogels carrying platelet gels for bone defect repair. *J Mater Chem B B* **2014**; 2: 8329-37. https://doi.org/10.1039/C4TB01356E
46. Bettencourt AF, Neves CB, de Almeida MS, Pinheiro LM, Oliveira SA, Lopes LP, *et al.* Biodegradation of acrylic based resins: A review. *Dent Mater* **2010**; 26: e171-80. https://doi.org/10.1016/j.dental.2010.01.006
47. Yi H, Ur Rehman F, Zhao C, Liu B, He N. Recent advances in nano scaffolds for bone repair. *Bone Res* **2016**; 4: 16050. https://doi.org/10.1038/boneres.2016.50
48. Yaghoubi Y, Movassaghpour A, Zamani M, Talebi M, Mehdizadeh A, Yousefi M. Human umbilical cord mesenchymal stem cells derived-exosomes in diseases treatment. *Life Sci* **2019**; 233: 116733. https://doi.org/10.1016/j.lfs.2019.116733
49. Wang L, Wang J, Zhou X, Sun J, Zhu B, Duan C, *et al.* A New Self-Healing Hydrogel Containing hucMSC-Derived Exosomes Promotes Bone Regeneration. *Front Bioeng Biotechnol* **2020**; 8: 564731. https://doi.org/10.3389/fbioe.2020.564731
50. Zhou J, Liu HX, Li SH, Gong YS, Zhou MW, Zhang JH, *et al.* Effects of human umbilical cord mesenchymal stem cells-derived exosomes on fracture healing in rats through the Wnt signaling

pathway. *Eur Rev Med Pharmacol Sci* **2019**; 23: 4954-60. https://doi.org/10.26355/eurrev_201906_18086

51. Zhang Y, Hao Z, Wang P, Xia Y, Wu J, Xia D, *et al.* Exosomes from human umbilical cord mesenchymal stem cells enhance fracture healing through HIF-1α-mediated promotion of angiogenesis in a rat model of stabilized fracture. *Cell Proliferation* **2019**; 52: e12570. https://doi.org/https://doi.org/10.1111/cpr.12570
52. Yang J, Chen Z, Pan D, Li H, Shen J. Umbilical Cord-Derived Mesenchymal Stem Cell-Derived Exosomes Combined Pluronic F127 Hydrogel Promote Chronic Diabetic Wound Healing and Complete Skin Regeneration. *Int J Nanomedicine* **2020**; 15: 5911-26. https://doi.org/10.2147/ijn.S249129.
53. Zinger O, Zhao G, Schwartz Z, Simpson J, Wieland M, Landolt D, *et al.* Differential regulation of osteoblasts by substrate microstructural features. *Biomaterials* **2005**; 26: 1837-47. https://doi.org/10.1016/j.biomaterials.2004.06.035
54. Luo Y, Engelmayr GC, Auguste DT, Ferreira L, Karp JM, Saigal R, *et al.*, eds. Chapter 24 – 3D Scaffolds. Academic Press; **2014**. https://doi.org/10.1016/B978-0-12-398358-9.00024-0